Available online at www.sciencedirect.com
SCIENCE DIRECT®
Surface Science 519 (2002) 90–100
SURFACE SCIENCE
www.elsevier.com/locate/susc

Lateral interaction and CO adlayer structures on the Pt(1 1 1) surface

N.V. Petrova, I.N. Yakovkin *

Institute of Physics, National Academy of Sciences of Ukraine, Prospect Nauki 46, Kiev 03028, Ukraine

Received 11 June 2002; accepted for publication 3 August 2002

Abstract

We have revisited the structures for CO films adsorbed on the Pt(1 1 1) surface and simulate the diffraction patterns. In particular, we suggest alternative placement of the CO molecules in the unit cell of the c(4 × 2) structure for CO on Pt(1 1 1) at $\theta = 0.5$. To correctly explain the LEED pattern, found from experiment at $\theta = 0.5$, the cell ultimately should be asymmetric. This agrees with recent STM results for similar CO structures on Ni(1 1 1). Parameters of the lateral interaction, evaluated from the Monte-Carlo simulations, are in excellent agreement with recent first-principle calculations. Formation of the stable CO adlayer structures on Pt(1 1 1) appears to be dominated by a superposition of the dipole–dipole and indirect interactions, which provide the attraction between the molecules at a characteristic spacing of $a\sqrt{3}$. Trio interactions are also found to be important and may originate from characteristic pairs of molecules in adsorption sites of different types.

Keywords: Monte Carlo simulations; Adsorption kinetics; Surface structure, morphology, roughness, and topography; Metallic surfaces; Platinum; Carbon monoxide

1. Introduction

CO oxidation reactions and adsorption have been one of the cornerstones of surface science. In spite of a great interest in CO adsorption on Pt surfaces, some essential aspects demand further investigations. It is well established that the CO oxidation on platinum surface occurs through the Langmuir–Hinshelwood mechanism, which makes the details of CO adsorption quite important in determining the oxidation reaction pathways and energetics [1]. The CO adsorption, perhaps, is the most widely studied on a close-packed Pt(1 1 1) surface [2–11]. Nevertheless, such essential issues as the adsorbed film structure and related lateral interaction between CO molecules, need elucidation.

The structures of various CO overlayers adsorbed on the Pt(1 1 1) surface have been extensively studied. Ertl et al. [2] reported that at coverage $\theta = 0.33$ the $(\sqrt{3} \times \sqrt{3})R30°$ structure was observed (θ is defined as the number of adsorbed CO molecules per Pt(1 1 1) surface atom). The corresponding LEED pattern is rather diffuse at $T = 170$ K while at $T = 160$ K, as reported in [3], it becomes sharp. At room temperature, the CO film is disordered [2,3]. However, Steininger et al.

* Corresponding author.
E-mail address: yakov@iop.kiev.ua (I.N. Yakovkin).

0039-6028/02/$ - see front matter
PII: S0039-6028(02)02199-4

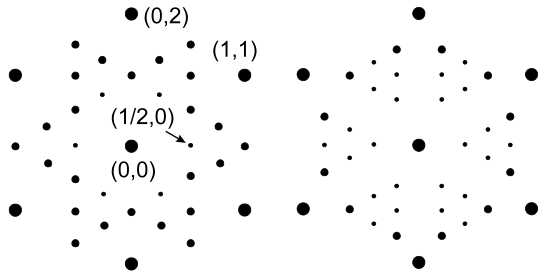

Fig. 1. Scheme of beams in LEED patterns for CO on Pt(1 1 1) at $\theta = 0.5$ and 0.6 [2,3]. Different sizes of the circles resemble the different intensities of the beams.

[4] claimed that on lowering the temperature to 100 K, the diffuse spots that could be attributed to the $(\sqrt{3} \times \sqrt{3})R30°$ structure got split into three beams, which should be attributed to some more complicated structure, visible even at $\theta = 0.17$. At $\theta = 0.5$, the LEED pattern (Fig. 1) reveals well developed film structure that remains sharp at room temperature [2–4]. According to notation suggested in [2], this structure is usually called c(4 × 2) [3–9]. It should be mentioned that the same LEED pattern for CO on Cu(1 1 1) was interpreted as a formation of the $(1.5 \times 1.5)R18°$ structure with a stoichiometry coverage 0.44 [12].

On the Ni(1 1 1) surface, the $(\sqrt{3} \times \sqrt{3})R30°$ structure at $\theta = 0.33$ and the c(4 × 2) structure at $\theta = 0.5$ also have been reported [13–19], but for higher coverages, the CO films acquire the $(\sqrt{7}/2 \times \sqrt{7}/2)R19.1°$ structure while, on Pt(1 1 1), the best resolved structure is the $c(5 \times \sqrt{3})$ rect-3CO at $\theta = 0.6$ (see Fig. 1). The $(\sqrt{3} \times \sqrt{3})R30°$ structure is also found for CO adsorbed on hexagonal faces of other transition metals such as Rh(1 1 1) [20–22] и Ru(0 0 0 1) [23,24], but for higher coverages the CO structures are different.

Because of a hexagonal structure of the Pt(1 1 1) surface, usually structures of adsorbed films are denoted in terms of the size and orientation of hexagonal lattices with respect to the substrate [2,20]. However, in many cases it is possible to choose a rectangular lattice for the adsorbed layer, and, in this case, more convenient is another notation that explicitly describes the size and type of the lattice and the number of particles in the unit cell [16]. Thus, the c(4 × 2) structure with 2 molecules per lattice site (which provides the $\theta = 0.5$ coverage) can be better described as $c(2 \times \sqrt{3})$ rect, with a molecule in the center of the cell, or as $(2 \times \sqrt{3})$ rect-2CO in general case. Then, the CO structure on Pt(1 1 1) at $\theta = 0.6$ (which, at $T = 170$ K, is approximately a saturation coverage [2–4]) in this notation will be $c(5 \times \sqrt{3})$ rect-3CO (see Fig. 1).

There is some controversy with regard to the type of adsorption sites occupied by CO molecules on the hexagonal transition metal surfaces [2,3,12–18]. For example, in Ref. [15], it has been found that CO molecules on Ni(1 1 1) occupy three-fold positions, while in Ref. [16], on-top and in-bridge positions have been convincingly argued. Concerning CO adsorption on the Pt(1 1 1), the situation seems more certain, and the most recognized is the model of occupation of the on-top sites at low coverages (up to $\theta = 0.33$ [3,5–10]) followed by occupation of the bridge sites. Redistribution of CO molecules over the sites with increasing coverage results in equal occupations of atop and bridge sites at $\theta = 0.5$ [3,5,24–26]. Such a sequential occupation of the adsorption sites follows from theoretical evaluations [6–10,25,26] as well as from results of IR spectroscopy for CO on Pt(1 1 1) [5]. Thus, in spite of all the efforts to-date, the details of the adsorption structure are not completely resolved, nor indeed are the mechanisms for lateral interactions between CO molecules in the overlayer.

It is well established that CO molecules on Pt(1 1 1) are oriented perpendicular to the surface with the carbon end down (see, e.g., [27] and references therein), and therefore dipole moments of the molecules should be parallel to each other. Hence, regardless to the origin of the dipole moment (that is, either resulted from the charge transfer to the substrate, which can be evaluated from initial decrease of the work function as $\mu \approx 0.2$ Debye [2,4], or due to inherent dipole moment of CO bond, 0.74 Debye for C–O and 2.3 Debye for C═O) one may expect a dipole–dipole repulsion between adsorbed molecules. The lateral repulsion between CO molecules on Pt(1 1 1) is evident from a decrease of the heat of adsorption on increasing coverage [2] and is supported by a number of theoretical evaluations [6–10,24–26]. On the other hand, formation of complicate structures as well as analysis of phase diagrams for

catalytic CO oxidation [28] indicates to attraction between adsorbed CO molecules at certain distances between them [7,23–26]. Obviously, the lateral attraction can be originated from indirect interactions [29,30], that is, mediated by the substrate electrons.

Hence, the lateral interaction between adsorbed CO molecules on the Pt(1 1 1) surface is of a complex non-monotonic character and depends on coverage. In this situation, interpretation of experimental results can be substantially improved by using a mathematical modeling [31–39]. Relevance of a mathematical model is determined both by ability of reproducing the major features of effects derived from experiments and by proximity of the model to realistic description of experimental conditions. For simulation of the catalytic CO oxidation on the platinum surface, the Ziff–Gullary–Barshad (ZGB) [40] algorithm is usually applied. This algorithm, however, has a number of shortcomings, which has initiated several ways of its improvement by including into consideration surface diffusion and lateral interactions [11,41–44]. In particular, by using a modified description of adsorption kinetics [11], it has become possible to avoid the poisoning of the Pt(1 1 1) surface by oxygen, which never appears in experiment while occurs in ZGB simulations, and to obtain the reaction rate dependencies on relative CO pressure in good agreement with experiment [11]. Nevertheless, for the case of CO adsorption (without oxygen on the surface), this algorithm still cannot provide a correct description of saturation CO coverages on the Pt(1 1 1) surface. Hence, the algorithm is to be improved to gain more realistic treatment of adsorption kinetics, which can be achieved by including into consideration the two types of adsorption sites on the Pt(1 1 1) surface and the indirect lateral interaction between adsorbed CO molecules. Such an improvement of the model is suggested in the present work.

2. Interpretation of LEED patterns for CO on Pt(1 1 1)

While the LEED pattern at $\theta = 0.33$ obviously corresponds to $(\sqrt{3} \times \sqrt{3})R30°$ CO film structure on Pt(1 1 1) or Ni(1 1 1) surface, interpretation of the patterns at $\theta = 0.5$ and at $\theta = 0.6$ (see Fig. 1) remains controversial [2–9]. Positions of beams in the LEED pattern indicate a two-dimensional lattice for the structure, but not positions of the molecules within the unit cell. The lattice that corresponds to the LEED pattern at $\theta = 0.5$, indeed can be denoted as $c(4 \times 2)$ or $(\sqrt{3} \times 2)$ rect, but for one molecule in the cell, the coverage will be $\theta = 0.25$ (Fig. 2(a)).

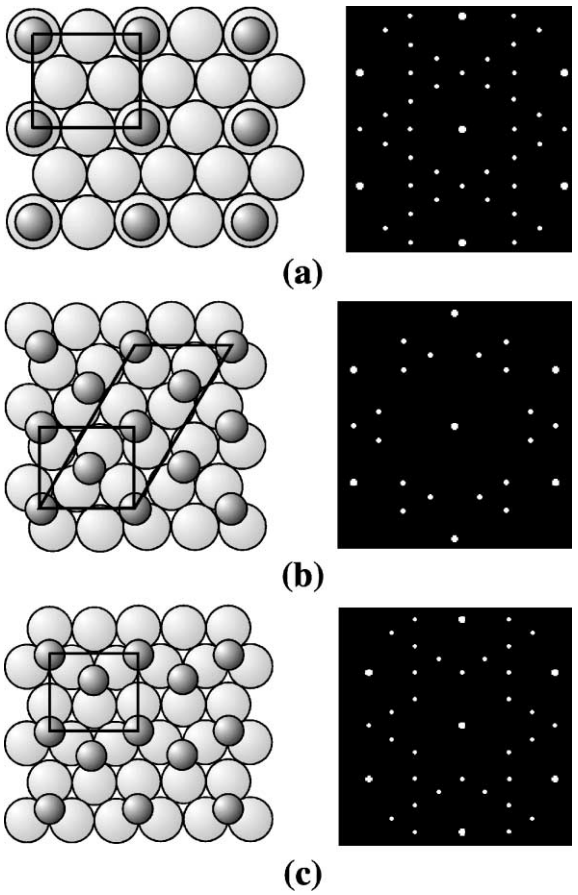

Fig. 2. (a) An important feature of the LEED pattern, calculated for three equivalent orientations for the $c(4 \times 2)$, or, in another notation, $(2 \times \sqrt{3})$ rect ($\theta = 0.25$) structure, is equivalence of intensities of all the six additional beams, forming characteristic triangles. (b) The $c(4 \times 2)$ structure, suggested for CO on Pt(1 1 1) [2] at $\theta = 0.5$ and calculated LEED pattern. (c) Structure, suggested for CO on Ni(1 1 1) [15] and calculated LEED pattern. Note the absence of certain beams in the (b) and (c) diffraction patterns, which are present in experiment.

Relative intensities of LEED reflections can be estimated within the kinematical approximation [32,45,46] as

$$I(h,k) = \left| \sum_n \exp\{2\pi i(hx_n + ky_n)\} \right|^2 \quad (1)$$

which yields a model LEED pattern (for example, such as shown in Fig. 2 (a)). Summation here is accomplished over occupied sites with x_n and y_n coordinates defined in terms of fractions of the "cell", which can be taken as the part of the surface under consideration, while h and k denote reciprocal space coordinates. For a hexagonal lattice, strong reflections appear when the sum of h and k is even (see Fig. 1). By taking arbitrary h and k, it is possible to simulate the distribution of LEED intensities over the screen (Fig. 2). This allows one to follow the transformations of the patterns with ordering the film structures and, if the step is small, also the changes in width of the beams resulted from decrease of the domain size. To this end, the part of the surface adopted in the present work, which contains 32×32 atoms of the Pt(1 1 1) surface, roughly corresponds to the area of 100×100 A [46], that is, to the coherence width for a routine LEED device. Such a choice facilitates the comparison of simulated LEED patterns with experiment.

To mimic the diffraction patterns, the LEED beams are depicted by circles whose sizes indicate the intensity, as evaluated according to Eq. (1). To improve clarity of the pictures, the beams that coincide with reflections generated by the substrate in LEED experiments, are marked by the circles of slightly increased size.

An important feature of the LEED pattern, calculated for three equivalent orientations for the c(4 × 2), or, in another notation, $(2 \times \sqrt{3})$ rect structure ($\theta = 0.25$), (Fig. 2(a)), is equivalence of intensities of all the six additional beams, forming characteristic triangles. It can be expected that additional molecules in the unit cell would diminish relative intensity for certain beams due to the structural factor. In particular, the (0.5,0) and other equivalent beams in the LEED pattern is noticeably weaker than the others (see Fig. 1(a)). Hence, this feature may serve as an indicator of reliability and correctness of suggested distribution of molecules in the unit cell. For example, in Fig. 2(b) and (c) are shown the structures, which were suggested for CO on Pt(1 1 1) [2] and CO on Ni(1 1 1) [14,15] at $\theta = 0.5$ (the scheme of the beams in this LEED pattern is shown in Fig. 1). As seen from the Fig. 2, calculated LEED patterns are substantially different from those obtained in experiment. It is due to position of the molecule in the center of the unit cell of the c(4 × 2) [2] structure (Fig. 2(b)) that some of beams, visible in experiment, are forbidden by the structural factor and therefore escape from the pattern. It should be noted also that the similar evaluation of relative intensities for this structure for CO on Ni(1 1 1) [15] has provided the same result. Certain beams (equivalent to (0.5,0)) are absent in the pattern also in the case of the shifting of the molecule from the cell center to another site on the symmetry line for the rectangle cell (Fig. 2(c)). It was claimed [15] that these beams could appear in LEED patterns due to multiple scattering effects, which, of course, could not be obtained within the kinematical approximation (which inclined the authors just to mark them in the calculated patterns). However, in experiment [2–4], these beams are only slightly weaker than the others, and therefore hardly could be attributed to the multiple scattering.

Hence, to gain the LEED pattern that agrees with experiment at $\theta = 0.5$, the CO molecule should be displaced from the symmetric position. To keep the equal occupation of bridge and atop sites [5], it is reasonable to consider the displacement of the molecule from the center of the rectangular unit cell to the neighboring bridge site, as suggested in Fig. 3(a). Such a choice of the site is almost unique because CO molecules are too large to occupy both an atop site and a nearest neighboring bridge site (minimum spacing between CO molecules on Pt(1 1 1) is about 3.2 Å [2,3], which substantially exceeds 1.38 Å, the distance between these sites), while the cell should be asymmetric to provide a correct LEED pattern. By reflecting the cell with respect to the mirror planes of the rectangle, other three unit cells of the $(2 \times \sqrt{3})$ rect-2CO structure can be obtained. Note that a sequential reflections in two planes result in the new cell that is equivalent to original one with

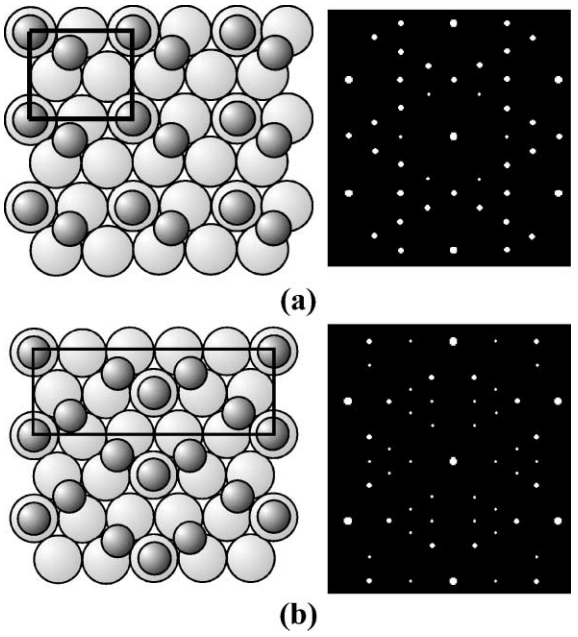

Fig. 3. (a) The $(2 \times \sqrt{3})$ rect-2CO structure with asymmetric unit cell, which is suggested for CO on Pt(1 1 1) at $\theta = 0.5$. The molecules in the corners of the rectangles occupy atop sites, while the others occupy bridge sites. Six equivalent domains of this structure (due to three possible lattice orientations for two mirror cells) provide the LEED pattern with noticeably decreased the (0.5,0) beam, in agreement with experiment. (b) The $c(5 \times \sqrt{3})$ rect-3CO structure of CO on Pt(1 1 1) at $\theta = 0.6$. Worth noting is addition of the third molecule to the characteristic "pair" of molecules in the bridge and atop sites spaced by characteristic $a\sqrt{3}/2$ distance.

regard to diffraction pattern. Thus, three equivalent lattice orientations for two mirror domain of the structure give rise to the LEED pattern (Fig. 3(a)), in excellent agreement with experiment. In particular, the (0.5,0) beam becomes noticeably decreased, but not as much as could be expected for the multiple scattering case.

In summary, the suggested model of the $(2 \times \sqrt{3})$ rect-2CO structure on the Pt(1 1 1) surface allows explanation of LEED patterns observed at $\theta = 0.5$, without referring to ghost multiple scattering effects. The suggested asymmetric unit cell is in line with recent STM results for a similar adsorption system CO/Ni(1 1 1) at $\theta = 0.5$. Indeed, the asymmetry of the unit cell is clearly visible in the STM pictures [16], in spite of the authors' explanation of the effect as an artifact.

For $\theta = 0.6$, the LEED pattern, which agrees with experiment, is obtained by summing the yields from six domains of the $c(5 \times \sqrt{3})$ rect-3CO structure, shown in the Fig. 3(b). The molecules in the center and in the angles of the unit cell occupy atop sites, while two additional molecules in the rectangular cell are in bridge sites. It is worth noting that this CO structure on the Pt(1 1 1) surface, which is seen at $\theta = 0.6$, can be obtained from the $(2 \times \sqrt{3})$ rect-2CO structure by adding the second bridge-site molecule to the pair of bridge-atop molecules (with $a\sqrt{3}/2$ spacing), while increasing the size of the lattice (Fig. 3(b)).

3. Simulation of structures formation by the Monte-Carlo technique

To form the $(\sqrt{3} \times \sqrt{3})R30°$ structure, at first glance, it could be sufficient to assume the dipole–dipole repulsion between adsorbed CO molecules [39], because this structure corresponds to maximum spacing between the molecules at $\theta = 0.33$. However, this structure is clearly seen at $T = 160$ K [2,3], which allows a rough evaluation of the critical temperature for the order–disorder transition of about 170 K. According to results of Monte-Carlo simulations, to gain such a high transition temperature, the dipole moment must be about 2 Debye, which hardly could be expected for the CO molecule on Pt(1 1 1). Hence, the lateral interaction between CO molecules should be of more complex character already at low coverages. The $(\sqrt{3} \times \sqrt{3})R30°$ structure, at $T = 100$ K, becomes visible at $\theta = 0.27$ [3], thus indicating the island formation, which implies attraction between the molecules for the $a\sqrt{3}$ spacing between them. It should be emphasized that this distance between CO molecules is characteristic for all film structures—$(\sqrt{3} \times \sqrt{3})R30°$, $(2 \times \sqrt{3})$ rect-2CO, and $c(5 \times \sqrt{3})$ rect-3CO (see Fig. 3), which evidently indicates to the minimum in potential of lateral interaction for the $a\sqrt{3}$ distance between the molecules.

More dense structures, $(2 \times \sqrt{3})$ rect-2CO and $c(5 \times \sqrt{3})$ rect-3CO, also reveal the complex lateral interaction with non-monotonic dependence on the distance between the molecules [6–8,24–26].

The indirect interaction through the substrate valence electrons is the most effective among the other types of lateral interactions that can give rise to attraction between molecules for such a long spacing as $a\sqrt{3}$ (4.8 Å) [29,30]. The potential of the indirect interaction, for not too small distances r between adsorbed molecules, oscillates with a period that depends on Fermi wave vector k_F of the substrate [29,30]:

$$V = \mathrm{Cr}^{-n}\cos(2k_F r + \delta) \quad (2)$$

Asymptotic of the potential is determined by n, which depends on the shape of Fermi surface and on existence of surface bands crossing the Fermi level. The latter case is the most favorable and provides the r^{-2} asymptotic, which makes the potential to be long-range indeed [30,47]. Obviously, in the case of transition metals, parameters in the Eq. (2)—amplitude C, Fermi vector k_F and the phase shift δ—will depend on direction and hardly could be evaluated rigorously. Therefore, it is reasonable to accept certain averaged values for the parameters, with subsequent adaptation them by using the Monte-Carlo approach. A tentative value of averaged Fermi wave vector for Pt can be taken about 1 Å^{-1} (for Au, similar evaluation gives $k_F = 1.2$ Å^{-1}), which leads to the period $\pi/k_F \approx 3.1$ Å. Then, by choosing $\delta = -0.1\pi$, position of the second minimum of the potential can be adjusted to the $a\sqrt{3}$ distance between CO molecules (Fig. 4). Lateral interaction between adsorbed molecules can be presented conveniently as a sum of a "direct" dipole–dipole repulsion and non-monotonic indirect interaction [30]. The result of such a summation is illustrated in Fig. 4(a). The dipole–dipole repulsion leads to the smoothing of the potential, of which the first minimum becomes "local", that is, the $a\sqrt{3}/2$ distance between CO molecules (which is characteristic for the couples of molecules in the $(2 \times \sqrt{3})$ rect-2CO structure, see Fig. 3(a)) is only slightly more favorable. It is not surprising therefore that at low coverages the $(2 \times \sqrt{3})$ rect-2CO structure is not formed. It should be noted also that for the CO molecule in a

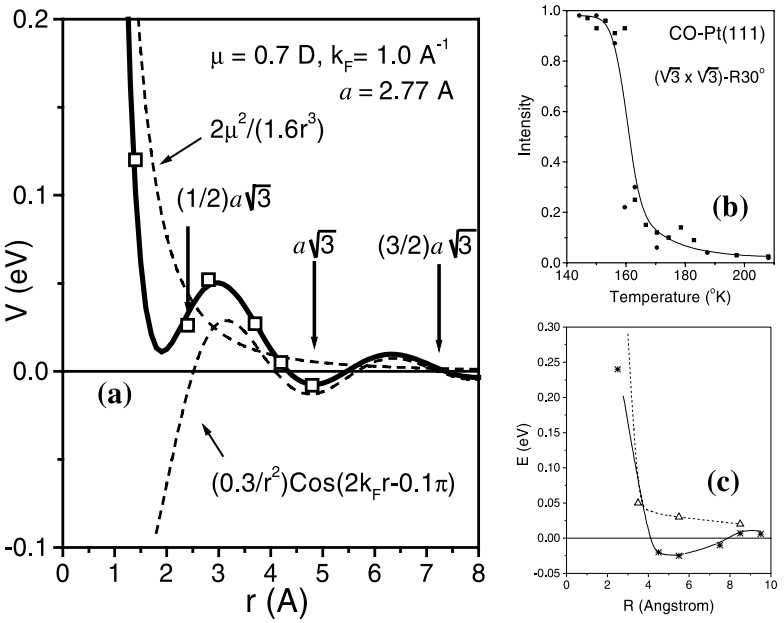

Fig. 4. (a) Dependence of the model potential of lateral interaction on the distance between CO molecules on Pt(1 1 1). Effective potential is a sum of the dipole–dipole and indirect interactions. Parameters values, chosen for the simulations, are denoted by symbols. (b) Simulated temperature dependence of intensity of the LEED beam for the $(\sqrt{3} \times \sqrt{3})R30°$ structure. (c) Energies of the lateral interactions calculated by Jennison et al. [7] for CO on Pt(1 1 1).

bridge site in the center of the rectangular cell, the distance from the corner molecules is 3.66 Å, which corresponds to the maximum in the potential. This feature immediately leads to conclusion that a centered unit cell must be unfavorable if one adopts the suggestion about the main role of the indirect interaction in forming the CO structures on Pt(1 1 1).

In the model used in the present work, the lateral interaction at $\theta = 0.33$ is described by the sum of dipole–dipole interaction $2\mu/r^3$ [29] and indirect interaction estimated from Eq. (2). Parameters of the interactions can be estimated by comparing results of Monte-Carlo simulations with data on disordering the $(\sqrt{3} \times \sqrt{3})R30°$ structure with increasing temperature. Thus, at $T = 160°$ K and $\theta = 0.33$, the LEED pattern for this structure is rather sharp, which indicates to a well ordered film structure [3]. At $T = 170°$ K, the brightness of the beams decreases, and, at room temperature, the CO films are disordered [2]. Values of parameters of lateral interaction, used in simulations of formation of the structures in present work, are denoted by symbols in Fig. 4(a), while Fig. 4(b) shows the temperature dependence of relative intensity of LEED beam for the $(\sqrt{3} \times \sqrt{3})R30°$ structure, obtained by Monte-Carlo simulation of order–disorder transition in CO films. As evident from the Fig. 4(a), the values of parameters of interaction for various distances between CO molecules on the Pt(1 1 1) surface indeed can be described by the sum of dipole–dipole and indirect interactions with $\mu = 0.7$ Debye and $C = 0.3$ eV Å^2.

As mentioned above, a sequential occupation of adsorption sites with increasing CO coverage on Pt(1 1 1) indicates to advantages of atop sites with respect to bridge sites. This feature can be assigned to more energetically favorable occupation of atop sites than bridge sites due to different adsorption bond strength for CO molecules in these sites. According to results quantum-chemical cluster calculations [25], the bond energy for the atop position of CO molecule on Pt(1 1 1) is 1.64 eV (which the value is close to 1.5 eV as derived from experiment [4]). In the bridge sites, the bond energy may be roughly estimated as to be of 10^{-2} eV lower than for atop sites [2,7]. Because of the two different types of adsorption sites at the surface, the lattice–gas model should be modified to account for the difference in adsorption energies for molecules in these sites. In the present work, the difference of the energies was simulated by the gain in energy of 0.01 eV when moving a molecule from a bridge site to an atop site.

For simulations of the formation of CO film structures, we used the matrix that contained 64 rows and 128 columns. To resemble a complex geometry of the sites lattice of the Pt(1 1 1) surface, 1/2 of thus introduced sites (that is, "ghost" sites) was excluded. Corresponding size of the simulated part of the surface, again, was approximately 100×100 Å, which provided sufficient statistics when averaging over particle distributions obtained for dynamical equilibrium conditions. It was assumed that such a part of surface resembled an infinite Pt(1 1 1) surface, hence, periodical boundary conditions were chosen.

The ordering of the film [32,33,40–42] was accomplished as follows. Initially, the particles were randomly distributed over the sites to resemble chosen coverage. Then randomly chosen particle moved to a neighboring site with probability $\exp(-\Delta E/kT)$. The energy difference were calculated with regard to the lateral interaction and the energy difference for two types of adsorption sites. In the case of a gain in energy ($\Delta E < 0$) due to the displacement, or when calculated probability exceeded a random number, the displacement was accomplished, while otherwise rejected. After 30–40 such displacements per particle, the dynamical equilibrium in the film was achieved, which could be controlled by evaluation of total energy (in equilibrium, the free energy approaches minimum while the total energy fluctuates about certain main value that depends on temperature).

If the temperature is lower than the critical temperature for the order–disorder transition in the film, there form domains of the structure related to chosen coverage, while for higher temperatures the film is disordered. Because the probability of displacement of the molecules is determined by the ratio $(-\Delta E/kT)$, the calculated transition temperature can be adjusted to experimental value by varying the parameters of the lateral interaction, which, in turn, allows their evaluation.

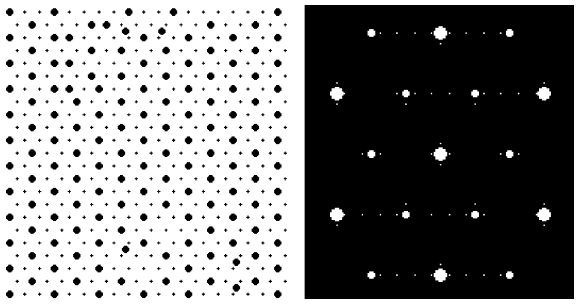

Fig. 5. A typical distribution of CO molecules over the sites on Pt(1 1 1) (snapshot) at equilibrium for $T = 160$ K and $\theta = 0.33$ (to left) and calculated LEED pattern (to right).

A typical equilibrium distribution (snapshot) of the molecules over the model surface, obtained at $\theta = 0.33$ and $T = 160$ K, is shown in Fig. 5. Formation of the $(\sqrt{3} \times \sqrt{3})R30°$ domain structure with separating boundaries ("domain walls") is evident. Majority of the molecules occupy atop sites, in agreement with experimental data for CO on Pt(1 1 1). The LEED pattern, calculated with using Eq. (1), also corresponds to one obtained in experiment [2].

It should be emphasized that the simulation has been conducted with using the values of interaction energy parameters, obtained from summing up the potentials of dipole–dipole and indirect interactions (see Fig. 4(a)). These values, denoted by symbols in Fig. 4(a), have been used then also in the simulations of order–disorder transition (Fig. 4(b)) and of formation of film structures at higher coverages, $\theta = 0.5$ and 0.6. Thus obtained parameters are in very good agreement with results of recent first-principle calculations [7] for energies of lateral interaction between CO molecules on the Pt(1 1 1) surface (see Fig. 4(c)). It should be noted that for explanation of the complex non-monotonic character of the lateral interaction [6], in particular, attraction between CO molecules at characteristic distances of 5–6 Å, no need to involve non-pairwise "trio" interactions, which believed previously to be unavoidable [7].

Presumably, trio interactions become important for formation of the $(2 \times \sqrt{3})$ rect-2CO structure. As seen in the Fig. 4(a), the first (local) minimum in the potential can provide appearance of the pairs of CO molecules situated in different (bridge–atop) sites at $a\sqrt{3}/2$ spacing. Formation of such pairs is a characteristic feature of the $(2 \times \sqrt{3})$ rect-2CO structure. Obviously, such a close location of the molecules should result in substantial redistribution of screening electron density. In other words, resulted potential can substantially deviate from the sum of potentials produced by individual molecules.

To account for the trio interactions, we used the following model description. In direction along the pairs, potential of the indirect interaction was reduced by switching off the attraction at the $a\sqrt{3}$ distance, which allowed a reasonable description of anisotropy of lateral interactions, characteristic for the $(2 \times \sqrt{3})$ rect-2CO structure.

The result of simulations for formation of this structure is illustrated by Fig. 6. To left, shown is a part of the 'snapshot' obtained after 40 jumps per particle, which reveals forming domains of the $(2 \times \sqrt{3})$ rect-2CO structure with certain orientation of the lattice. Corresponding LEED pattern, calculated for three possible orientations of the lattice (in experiment, the size of the electron beam usually much exceeds both the coherence width and domain size), is presented in the right panel of Fig. 6.

Hence, for formation of domains of single orientation of the $(2 \times \sqrt{3})$ rect-2CO structure, essential is the appearance of the characteristic pairs of CO molecules, which may serve as cores for the domain growth. These pairs "switch on" the trio interactions which provide the anisotropy of lateral interaction. Such cores may appear at random, as in the case illustrated by Fig. 6, or can be

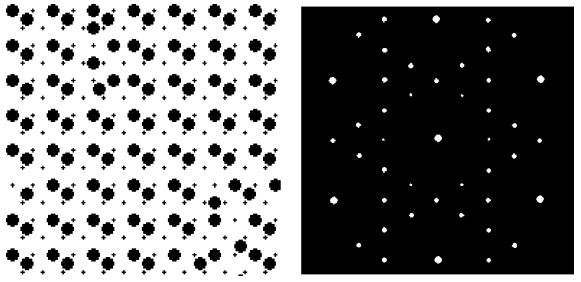

Fig. 6. Results of simulations for formation of the $(2 \times \sqrt{3})$ rect-2CO structure. Presented are a snapshot at equilibrium for $T = 300$ K and $\theta = 0.5$ and calculated LEED pattern.

introduced explicitly to simulate atomic steps on real surface.

4. Kinetics of CO adsorption on Pt(1 1 1)

The most important disagreement between ZGB simulations of CO oxidation on Pt surfaces [40–44] and experimental results is the value of saturation CO coverage. The $\theta = 1$ coverage ultimately results from the ZGB algorithm, while experiment gives $\theta = 0.5$ at room temperature. Presumably, this controversy may be attributed to inadequate description of lateral interaction as well as to oversimplified description of the Pt(1 1 1) surface by a lattice of single-type sites. Both these shortcomings have been removed from the model suggested in the present study, which can provide more realistic interpretation of the CO adsorption kinetics.

Our "real-time" algorithm for simulations of gas adsorption has been described in detail elsewhere [36], therefore here we will outline only the main features relevant for present study of kinetics of CO adsorption on Pt(1 1 1). For constant CO pressure, the flux of impinging molecules can be expressed in terms of a fraction of monolayer per second (that is, the coverage, provided that the sticking coefficient would be unity). This allows a definition of the exposition, which may be expressed right in Langmuirs, and thus facilitates comparison with adsorption isobars, obtained in experiment.

According to experiment [48,49], initial sticking coefficient for CO on the Pt(1 1 1) surface was taken to be 0.9. In the model, this feature was simulated by related probability (0.9) of adsorption on a randomly chosen site on a clean surface (regardless the lateral interaction). The extrinsic precursor states were accounted for by increasing probability of capturing when a CO molecule impinged already occupied site. In this case, the molecule was allowed to occupy a neighboring vacant site. This algorithm implicitly accounts for enhanced sticking probability due to better mass match for collisions of impinging CO molecules with adsorbed molecules than with a bare Pt(1 1 1) surface.

The adsorption step (certain adsorption "time interval") is followed by the ordering of the film, as described in the previous section, and by desorption events, of which the number depends on the time interval. It is assumed that the desorption probability is determined from Polani–Wigner equation with activation energy dependent on lateral interaction and type of adsorption site [36,49]. Such an algorithm has been proved valid for correct description of kinetics of molecular hydrogen adsorption on the W(1 1 0) surface [36]. Specifically, both coverage dependence of sticking and saturation coverages, attained for various molecular fluxes and temperatures, have been addressed in good agreement with experiment.

Results of simulations of kinetics of adsorption for CO on Pt (1 1 1) are presented in Fig. 7. At low coverages, the sticking coefficient is almost constant (Fig. 7(a)), which resembles its behavior known from experiment [2,4,48,49] and indicates to correctness of the adopted description of the precursor states in the present model. As the cov-

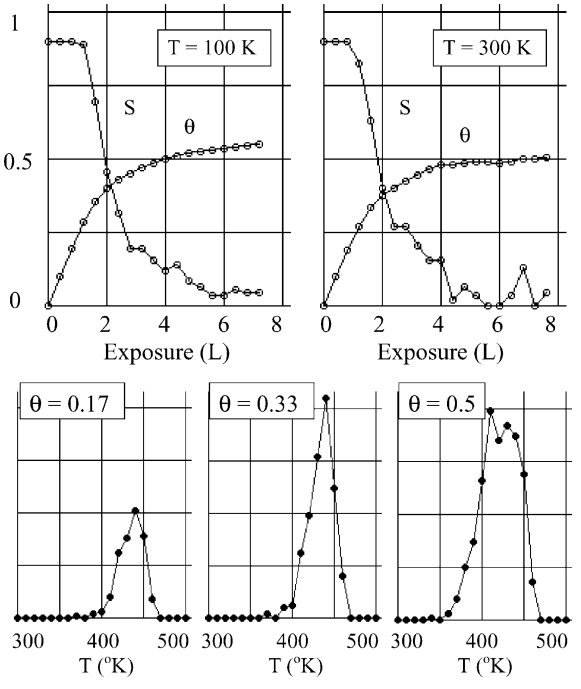

Fig. 7. Calculated dependences of the sticking coefficient S and coverage θ on CO exposure and simulated TPD spectra for CO on Pt(1 1 1).

erage further increases, S rapidly decreases due to repulsive fraction of the lateral interaction and decreasing number of vacant adsorption sites on the surface. At $T = 300$ K, dynamical equilibrium between adsorption and desorption is achieved at coverage about 0.5, while in the case of adsorption on the cooled ($T = 100$ K) surface, the coverage continues to increase slowly and approximates $\theta = 0.6$ value, in agreement with experiment.

By using a routine Monte-Carlo approach for simulations of temperature-programmed desorption (TPD) spectra [36–38], with keeping the same parameters of lateral interaction, the TPD spectra for CO on Pt(1 1 1) also can be reproduced, in agreement with experiment [4] (Fig. 7). To facilitate comparison with experiment [4], adsorption of CO was modeled at $T = 100$ K and finished when the certain coverage (specifically, 0.17, 0.33 and 0.5) was achieved. Then the temperature was stepwise increased to mimic linear increase with the rate of 15 K/s, and relative number of desorbed molecules at each step resembled the desorption rate. Thus, for $\theta = 0.17$, when the lateral interaction is negligible and most of the molecules are in atop sites, there is a single maximum in the spectrum at $T = 480$ K. For higher coverages, there appears a low-temperature shoulder which reveals increasing role of the lateral interaction as well as partial occupation of bridge adsorption sites.

Hence, obtained by modeling, coverage dependences of sticking and saturation coverages for CO on the Pt(1 1 1) surface, at various temperatures, are in good agreement with experiment [2–4,48,49]. Kinetics parameters (desorption activation energy $E_d = 1.2$ eV for frequency factor $\nu = 10^{13}$ s^{-1}), used in the simulations, also agree well with evaluations reported in Refs. [2,4–9,49].

5. Conclusions

Suggested models of structures of CO films on the Pt(1 1 1) surface do explain LEED patterns reported for this system at various coverages and temperatures. In particular, at $\theta = 0.5$, the unit cell of the $(2 \times \sqrt{3})$ rect-2CO film structure is found to be asymmetric, in contrast to previously suggested centered cell of the c(4 × 2) (or c$(2 \times \sqrt{3})$ rect) structure. Despite of equal occupation of bridge and atop sites by CO molecules and equivalent lattices, these structures are different with regard to the structural factor, which results in diminishing of certain beams for the centered cell, while the suggested $(2 \times \sqrt{3})$ rect-2CO structure resembles the LEED pattern in agreement with experiment. The asymmetry of the unit cell at $\theta = 0.5$ is in line with recent STM results [16] for a similar adsorption system CO/Ni(1 1 1) as well.

A complex non-monotonic lateral interaction between adsorbed CO molecules can be attributed to superposition of the dipole–dipole and indirect interactions through the electrons at the Pt(1 1 1) surface, which results in effective attraction for spacing of $a\sqrt{3}$ inherent for CO structures, and in appearance of a local minimum in potential at $a\sqrt{3}/2$. This minimum leads to formation of characteristic pairs of the molecules, which may switch on the trio interactions that are essential for formation of the $(2 \times \sqrt{3})$ rect-2CO and c$(5 \times \sqrt{3})$ rect-3CO structures. Values of parameters of the lateral interaction, obtained through Monte-Carlo simulations, are in very good agreement with results of recent first-principle calculations [7].

Simulated coverage dependences of sticking coefficient and saturation coverages for CO on the Pt(1 1 1) surface, are in good agreement with experiment [2–4,48,49]. In particular, due to improved description of the lateral interaction and of two different types of adsorption sites, as well as due to proper account for the role of extrinsic precursor states, correct saturation CO coverage $\theta = 0.5$ at $T = 300$ K has been obtained. We hope that suggested interpretation of the CO structures and evaluation of parameters of lateral interaction will be useful for further investigations of catalytic CO oxidation on Pt(1 1 1) surface, while the developed algorithm may be explored for more realistic simulations of the reaction.

Acknowledgements

The authors would like to acknowledge helpful discussions with Yu.G. Ptushinskii and P.A. Dowben, with gratitude for critical reading of the manuscript.

References

[1] R. Imbihl, Prog. Surf. Sci. 44 (1993) 185.
[2] G. Ertl, M. Neumann, K.M. Streit, Surf. Sci. 64 (1977) 393.
[3] P.R. Norton, J.A. Davies, T.E. Jackman, Surf. Sci. Lett. 122 (1982) L593.
[4] H. Steininger, S. Lehwald, H. Ibach, Surf. Sci. 123 (1982) 264.
[5] B.N.J. Persson, R. Ryberg, Phys. Rev. B 40 (1989) 20173.
[6] D.C. Skelton, D.H. Wei, S.D. Kevan, Surf. Sci. 320 (1994) 77.
[7] D.R. Jennison, P.A. Schultz, M.P. Sears, Phys. Rev. Lett. 77 (1996) 4828.
[8] R. Brako, D. Sokcevic, Surf. Sci. 401 (1998) L388.
[9] K.L. Kostov, P. Jakob, D. Menzel, Surf. Sci. 377–379 (1997) 802.
[10] F. Debecq, Surf. Sci. 389 (1997) L1131.
[11] I.N. Yakovkin, V.I. Chernyi, A.G. Naumovets, Surf. Sci. 442 (1999) 81.
[12] P. Hollins, J. Pritchard, Surf. Sci. 99 (1980) L389.
[13] K. Chrestmann, O. Schober, G. Ertl, J. Chem. Phys. 60 (1974) 4719.
[14] H. Conrad, G. Ertl, J. Kuppers, E.E. Latta, Surf. Sci. 57 (1976) 475.
[15] L. Becker, S. Aminpirooz, B. Hillert, M. Pedio, J. Haase, D.L. Adams, Phys. Rev. B 47 (1993) 9710.
[16] N. Ikemiya, T. Suzuki, M. Ito, Surf. Sci. 466 (2000) 119.
[17] R. Davis, R. Toomes, D.P. Woodruff, O. Schaff, V. Fernandez, K.-M. Schindler, Ph. Hofmann, K.-U. Weiss, R. Dippel, V. Fritzsche, A.M. Bradshaw, Surf. Sci. 393 (1997) 12.
[18] L.D. Mapledoram, M.P. Bessent, A. Wander, D.A. King, Chem. Phys. Lett. 228 (1994) 527.
[19] L. Surnev, Z. Xu, J.T. Yates, Surf. Sci. 201 (1988) 1.
[20] M. Giere, A. Barbieri, M.A. Van Hove, G.A. Somorjai, Surf. Sci. 391 (1997) 76.
[21] D.H. Wei, D.C. Skelton, S.D. Kevan, Surf. Sci. 381 (1997) 49.
[22] M. Beutl, J. Lesnik, K.D. Rendulic, Surf. Sci. 429 (1999) 71.
[23] B. Reidmuller, I.M. Ciobica, D.C. Papageorgopoulos, B. Berenbak, R.A. van Santen, A.W. Kleyn, Surf. Sci. 465 (2000) 347.
[24] J.J. Mortensen, B. Hammer, J.K. Norskov, Surf. Sci. 414 (1998) 315.
[25] Y. Morikawa, J.J. Mortensen, B. Hammer, J.K. Norskov, Surf. Sci. 386 (1997) 67.
[26] H. Aizawa, S. Tsuneyuki, Surf. Sci. 399 (1998) L364.
[27] P.A. Dowben, B. Xu, J. Choi, E. Morikawa, in: H.S. Nalwa (Ed.), Handbook of Thin Film Materials, Characterization and Spectroscopy of Thin Films, vol. 2, Academic Press, 2002, p. 61.
[28] N. Pavlenko, P.P. Kostrobij, Yu. Suchorski, R. Imbihl, Surf. Sci. 489 (2001) 29.
[29] T.L. Einstein, CRC Crit. Rev. Sol. St. Mater. Sci. 7 (1978) 261.
[30] O.M. Braun, V.K. Medvedev, Sov. Phys. Usp. 32 (1989) 328.
[31] T.T. Tsong, Surf. Sci. 122 (1982) 99.
[32] J. Kuppers, Vacuum 21 (1971) 393.
[33] I.N. Yakovkin, Surf. Sci. 282 (1993) 195.
[34] I. Hasegawa, S. Ino, Phys. Rev. Lett. 68 (1992) 1192.
[35] P. Schad, S. Heun, T. Heidenblut, M. Henzler, Phys. Rev. B. 45 (1992) 11430.
[36] N.V. Petrova, I.N. Yakovkin, Yu.G. Ptushinskii, Surf. Sci. 497 (2002) 349.
[37] B. Lehner, M. Hohage, P. Zeppenfeld, Surf. Sci. 454–456 (2000) 251.
[38] B. Meng, W.H. Weinberg, J. Chem. Phys. 100 (1994) 5280.
[39] K. Fichthorn, E. Gulari, R. Ziff, Surf. Sci. 243 (1991) 273.
[40] R.M. Ziff, E. Gulary, Y. Barshad, Phys. Rev. Lett. 24 (1986) 2553.
[41] J. Mai, W. von Niessen, A. Blumen, J. Chem. Phys. 93 (1990) 3685.
[42] R. Chakarova, Surf. Sci. 389 (1997) 234.
[43] L.M. Sander, S.V. Ghaisas, Surf. Sci. 391 (1997) 125.
[44] M. Ehsasi, M. Matloch, O. Frank, J.H. Block, J. Chem. Phys. 91 (1989) 4949.
[45] L.D. Roelofs, R.L. Park, T.L. Einstein, J. Vac. Sci. Technol. 16 (1979) 478.
[46] V.K. Medvedev, I.N. Yakovkin, Sov. Phys. Sol. St. 19 (1977) 1515.
[47] O.M. Braun, L.G. Ilchenko, E.A. Pashitsky, Sov. Phys. Sol. St. 22 (1980) 1649.
[48] I.N. Yakovkin, V.I. Chernyi, A.G. Naumovets, J. Phys. D: Appl. Phys. 32 (1999) 841.
[49] M. Kiskinova, G. Pirug, H.P. Bonzel, Surf. Sci. 133 (1983) 321.